Technical Note: Signal Generator Models

Paul F. Roysdon, Ph.D.

I. Inertial Measurement Unit Model

A. IMU Background and Notation

The Signal Generator models a triad (i.e. 3-axes) angular rate sensor (gyroscope) and a triad linear acceleration sensor (accelerometer). Thus providing measurements related to three-dimensional (3D) body-fixed spatial behavior.

When evaluating an IMU for a specific INS application, one must consider a few key IMU parameters which have an effect on the system-level position, velocity and attitude accuracy. The general form of the equation which represents a single axis sensor (e.g. single-axis gyro), is:

$$y_i(t) = (1 + \epsilon_k) \cdot [u_i(t) + \omega_i(t) + \eta_{MA} + \eta_Q + \cdots] \quad (1)$$

where $y_i(t)$ is the result of input $u_i(t)$, which is multiplied by some Scale Factor ϵ_k, and summed with a random bias $\omega_i(t)$, Misalignment η_{MA}, Quantization Noise η_Q, Rate Random Walk η_{RRW}, Rate Ramp η_{RR}, etc.. Errors like Scale Factor and Misalignment are fixed, given by the manufacturer, and are typically part of the sensor calibration. Whereas, Random Walk and Bias Instability (both are contained in $\omega_i(t)$) are random, will cause errors to accumulate over time, and thus need to be characterized and modeled.

The biases, with units which are commonly found on manufacturer data sheets [1] and Allan Variance values defined in [4], are summarized in Table II, while Figure 1 provides an intuitive flow chart of the errors, with the parameters defined in Table I.

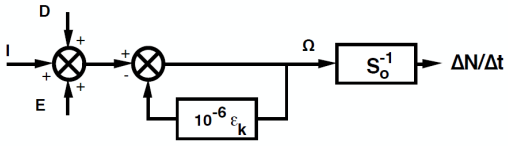

Fig. 1. Generic IMU Model [4]

TABLE I
GENERIC IMU MODEL PARAMETERS [4]

Symbol	Definition
$S_0(\Delta N/\Delta t)$	$[I + E + D](1 + 10e^{-6}\epsilon_k)^{-1}$
S_0	Nominal scale factor
$\Delta N/\Delta t$	Output pulse rate
I	Inertial input terms
E	Environmentally sensitive terms
D	Drift terms
ϵ_k	Scale factor error terms (ppm)
Ω	Equivalent gyro rate output

TABLE II
SENSOR ERRORS

Symbol	Interpretation	$S_{\tilde{Y}}(j\omega)$	Units
Gyro Channels			
g_{bo}	Initial Bias	$B_o^2\delta(f)$	deg/hr
g_b	In-run Bias Stability	$\frac{B^2}{2\pi f}$	deg/hr
g_{RW}	Random Walk	N^2	deg/$\sqrt{hr}$
g_{SF}	Scale Factor	-	ppm
g_{MA}	Misalignment	-	deg
g_Q	Quantization	$\frac{4Q^2}{\tau} sin^2 \pi f \tau$	-
g_{RRW}	Rate Random Walk	$\frac{K^2}{(2\pi f)^2}$	-
g_{RR}	Ramp Instability	$\frac{R^2}{(2\pi f)^3}$	-
Accelerometer Channels			
a_{bo}	Initial Bias	$B_o^2\delta(f)$	milli-g
a_b	In-run Bias Stability	$\frac{B^2}{2\pi f}$	μ-g
a_{RW}	Random Walk	N^2	μ-g/$\sqrt{hr}$
a_{SF}	Scale Factor	-	ppm
a_{MA}	Misalignment	-	deg
a_Q	Quantization	$\frac{4Q^2}{\tau} sin^2 \pi f \tau$	-
a_{RRW}	Rate Random Walk	$\frac{K^2}{(2\pi f)^2}$	-
a_{RR}	Ramp Instability	$\frac{R^2}{(2\pi f)^3}$	-

B. Initial Bias Error

Bias Error consists of two components: initial offset called *Initial Bias* (also called called *turn-on to turn-on bias*), and long-term random drift called *In-run Bias Stability* (also called *Flicker Noise*). Because Initial Bias is calibrated from the manufacturer, and not determined from the Allan Variance, we need only consider In-run Bias Stability.

C. In-run Bias Stability Error

In-run Bias Stability is the random variation in the bias. This parameter provides the benchmark of the best that is achievable for a selected sensor in terms of bias variation for a fully modeled system without aiding from other sensors. In-run Bias Stability is an indication of angle, or velocity, error which increases proportionally with time. The resulting angle error (gyro) introduces a misalignment of the IMU orientation, affecting the projection of the gravity vector and linear acceleration. The resulting velocity error (accelerometer) effects both linear acceleration as well as the sensors ability to measure the gravity vector. These results combine in velocity errors which increase with t^2, and position error which increase with t^3.

D. Random Walk Error

Random Walk is the unwanted signal generated from internal electronics that interfere with the measurement of the desired signal. The noise level will determine the minimum

sensor output which is distinguishable from the background noise of the sensor, or noise floor. Random Walk is a common specification used to quantify sensor white noise output for a given sensor bandwidth. Random Walk will affect the projection of the gravity vector, as well as the position and velocity estimates. The gyro ARW is defined as

$$\sigma^2(\tau) = \frac{N^2}{\tau} \tag{2}$$

Re-arranging the above equation for N, we find:

$$N = \sigma(\tau)\sqrt{\tau} \tag{3}$$

The coefficient N is the ARW and can be determined from the Allan Deviation plot by choosing the value which corresponds to $\tau = 1$.

II. Global Positioning System Model

The Signal Generator uses Receiver Independent Exchange (RINEX) [11] files downloaded from a Continuously Operating Reference Station (CORS) [10] server, such that real satellite orbits can be produced for any given day. For a specified trajectory, GPS "ground truth" and noise corrupted measurements of both L1 & L2 pseudorange, Doppler, and carrier phase are produced. Measurement errors include: troposphere, ionosphere, and multipath delay, as well as thermal noise, GPS receiver clock bias and clock drift.

A. Pseudorange Observable

The L1 and L2 pseudorange measurements for the i-th satellite at time t are modeled as

$$\begin{aligned}\tilde{\rho}^i_{r_1}(t) &= \|\mathbf{p}_r(t) - \mathbf{p}^i(t)\|_2 + c\delta t_r(t) \\ &\quad + \frac{f_2}{f_1} I^i_r(t) + T^i_r(t) + M^i_{\rho_1}(t) + n^i_{\rho_1}(t), \end{aligned} \tag{4}$$

$$\begin{aligned}\tilde{\rho}^i_{r_2}(t) &= \|\mathbf{p}_r(t) - \mathbf{p}^i(t)\|_2 + c\delta t_r(t) \\ &\quad + \frac{f_1}{f_2} I^i_r(t) + T^i_r(t) + M^i_{\rho_2}(t) + n^i_{\rho_2}(t), \end{aligned} \tag{5}$$

where

- $\|\mathbf{p}_r - \mathbf{p}^i\|_2$ is the geometric distance between the rover position $\mathbf{p}_r \in \mathbb{R}^3$ and the i-th satellite vehicle position $\mathbf{p}^i \in \mathbb{R}^3$,
- $c = 2.99792458 \times 10^8\ m/s$ is the speed of light,
- $\delta t_r \in \mathbb{R}$ is the receiver clock bias which is identical to all channels of the receiver,
- $f_1 = 1575.42MHz$ is the L1 carrier frequency,
- $f_2 = 1227.60MHz$ is the L2 carrier frequency,
- I^i_r is the Ionospheric error due to dispersive atmospheric effects in the layer of the atmosphere with altitude between 50 and 1000 km,
- T^i_r is the Tropospheric error due to non-dispersive atmospheric effects in the lower part of the atmosphere extending from the surface to 50 km above the surface of the planet,
- $M^i_{\rho_1}$ and $M^i_{\rho_2}$ are the pseudorange multipath errors caused by signal reflections,
- $n^i_{\rho_1},\ n^i_{\rho_2} \sim \mathcal{N}(0, {\sigma^i_\rho}^2)$ are the (non-common mode) pseudorange measurement noise.

B. Carrier Phase Observable

The L1 and L2 carrier phase measurements $\tilde{\varphi}^i_{r1}$ and $\tilde{\varphi}^i_{r2}$ for the i-th satellite at time t are modeled as

$$\begin{aligned}\lambda_1\tilde{\varphi}^i_{r1}(t) &= \|\mathbf{p}_r(t) - \hat{\mathbf{p}}^i(t)\|_2 + c\delta t_r(t) + \lambda_1 N^i_1(t) \\ &\quad + E^i_{cm3}(t) + M^i_{\varphi_1}(t) + n^i_{\varphi_1}(t), \end{aligned} \tag{6}$$

$$\begin{aligned}\lambda_2\tilde{\varphi}^i_{r2}(t) &= \|\mathbf{p}_r(t) - \hat{\mathbf{p}}^i(t)\|_2 + c\delta t_r(t) + \lambda_2 N^i_2(t) \\ &\quad + E^i_{cm4}(t) + M^i_{\varphi_2}(t) + n^i_{\varphi_2}(t), \end{aligned} \tag{7}$$

where

- λ_1 and λ_2 are the wavelength of the corresponding carrier signals,
- N^i is the ambiguous integers representing the unknown number of whole cycles,
- E^i_{cm3} and E^i_{cm4} are common mode errors similar to E^i_{cm1} and E^i_{cm2} detailed in Section II-A

$$E^i_{cm3} = E^i + c\delta t^i - \frac{f_2}{f_1} I^i_r + T^i_r, \tag{8}$$

$$E^i_{cm4} = E^i + c\delta t^i - \frac{f_1}{f_2} I^i_r + T^i_r, \tag{9}$$

- $M^i_{\varphi_1},\ n^i_{\varphi_1},\ M^i_{\varphi_2},\ n^i_{\varphi_2}$ are non-common mode errors similar to those of pseudorange measurements.

C. Delta Pseudorange Observable

The Delta Pseudorange observable, often referred to as the Doppler observable, is actually a quantity of subsequent pseudorange measurements over a consecutive time interval.

The Doppler frequency can be expressed as

$$f_r = f_T \left(1 - \frac{\dot{R}}{c}\right) \tag{10}$$

relates the frequency received by a user f_r to the rate of change of the range between the receiver and the transmitter, where f_T is the transmitted frequency, and $\dot{R}$ is the geometric range between the user and the transmitter. The Doppler shift is

$$f_r - f_T = f_T \frac{\dot{R}}{c}. \tag{11}$$

In GPS receivers, the delta pseudorange is a measurement of the quantity

$$\Delta\rho(\tau_r(t)) = \rho^s_r(\tau_r(t)) - \rho^s_r(\tau_r(t) - T) \tag{12}$$

where typically $T \leq 1.0$. This quantity is the change in range over the time interval $\tau_r \in [\tau_r(t) - T, \tau_r(t)]$:

$$\Delta\rho(\tau_r(t)) = \int_{\rho^s_r(\tau_r(t)-T)}^{\rho^s_r(\tau_r(t))} \dot{\rho}^s_r(q)dq. \tag{13}$$

Therefore, if the delta pseudorange is divided by T it measures the average rate of change of the pseudorange over the

indicate time interval. By the mean value theorem, there is a value of $q \in [\tau_r(t)-T, \tau_r(t)]$ such that $\dot{\rho}_r^s(q) = \frac{1}{T}\Delta\rho(\tau_r(t))$. By this reasoning the delta pseudorange observable is often modeled as the rate of change of the pseudorange at the midpoint of the interval $\tau_r \in [\tau_r(t) - T, \tau_r(t)]$ and referred to as the Doppler observable.

Assuming that the receiver has and maintains phase lock over the interval $\tau_r \in [\tau_r(t) - T, \tau_r(t)]$ that is of interest, then the Doppler observable can be computed as

$$\Delta\rho(\tau_r(t)) = \lambda\left(\phi_r^i(\tau_r(t)) - \phi_r^i(\tau_r(t) - T)\right). \tag{14}$$

It is reasonable to assume that the measurement of the Doppler shift (in Hz) at the receiver indicated time is

$$D(\tau_r(t)) = \frac{\Delta\rho(\tau_r(t))}{\lambda T}. \tag{15}$$

The Doppler measurement model is

$$\begin{aligned}\lambda T D_r^s(\tau_r(t)) = (\rho_r^s(\tau_r(t)) - \rho_r^s(\tau_r(t) - T)) \\ - c\Delta\dot{t}^i + \epsilon(\tau_r(t)).\end{aligned} \tag{16}$$

where the temporal differences for E^i, I_r^i, and T_r^i have been dropped because they are small relative to the other terms, $\epsilon(\tau_r(t))$ represents the measurement error due to multipath and receiver noise, and $\Delta\dot{t}^i = \Delta t^i(\tau_r) - \Delta t^i(\tau_r - T)$ is the (uncorrected) satellite clock drift rate. The symbol $\Delta\dot{t}^i$ is used instead of $\delta\dot{t}^i$ as a reminder to correct the Doppler measurement for the satellite clock drift rate.

Assuming that the line-of-sight vector from the satellite to the user, $\mathbf{h}^\intercal$, is available from the position solution, a linearized model for the Doppler measurement is

$$\lambda D_r^s = \mathbf{h}^\intercal(\mathbf{v}_r - \mathbf{v}^s) + c\Delta\dot{t}_r - c\Delta\dot{t}^i + \epsilon. \tag{17}$$

where $\mathbf{v}_r$ is the velocity of the receiver, and $\mathbf{v}^s$ is the s-th satellite velocity. The satellite velocity computation is described in Section C.4 of [3]. The satellite clock drift rate $c\Delta\dot{t}^i$ is predicted by the broadcast model to be $a_{f1}T$, see Section C.1 of [3].

D. Other models

GPS antenna separation from an INS may be specified in $\delta p = \{\delta x, \delta y, \delta z\}$, to model antenna to INS separation effects.

GPS antenna beam-width, may be specified to model pitch & roll drop-out effects on GPS-INS performance.

Loss-of-lock due to acceleration may be specified to model G-sensitive effects.

III. Trajectory Generator

The trajectory generator uses kinematic equations (i.e. angular rates and specific forces) to integrate a trajectory "ground truth", such that position, velocity, and attitude are produced, in three reference frames: Earth Centered Inertial (ECI), Earth Centered Earth Fixed (ECEF), Local Tangent Plane North East Down (NED).

Let $\mathbf{x} \in \mathbb{R}^{n_s}$ denote the rover state vector, where

$$\mathbf{x}(t) = [\mathbf{p}^\intercal(t), \mathbf{v}^\intercal(t), \boldsymbol{q}^\intercal(t)]^\intercal \in \mathbb{R}^{n_s},$$

where $\mathbf{p}$, $\mathbf{v}$, each in $\mathbb{R}^3$ represent the position, and velocity vectors, respectively, and $\boldsymbol{q}$ represents the attitude quaternion. In this example, $n_s = 10$. If an Euler representation were used, then $n_s = 9$.

The kinematic equations for the rover state are

$$\dot{\mathbf{x}}(t) = \boldsymbol{f}(\mathbf{x}(t), \boldsymbol{u}(t)), \tag{18}$$

where $\boldsymbol{f} : \mathbb{R}^{n_s} \times \mathbb{R}^6 \mapsto \mathbb{R}^{n_s}$ represents the kinematics, and $\boldsymbol{u} \in \mathbb{R}^6$ is the vector of specific forces and angular rates. The function $\boldsymbol{f}$ is accurately known (see Chapter 11 in [3]). The simulation integrates eqn. (18) to produce $\mathbf{x}(t)$, from the prior for the first state: $\mathbf{x}(t_0)$.

Let $t_k = kT$ denote the time instants at which GPS measurements are valid. Let τ_i denote the time instants at which IMU measurements are valid. It is typically the case that $T \gg [\tau_i - \tau_{i-1}]$. Therefore, there are numerous IMU measurements available between GPS epochs. For a variable $a(t)$, to simplify notion, define $a_i \triangleq a(\tau_i)$ and $a_k \triangleq a(t_k)$. Define $\mathbf{U}_k \triangleq \{\tilde{\mathbf{u}}_i | \tau_i \in [t_{k-1}, t_k]\}$

The solution of (18) over the interval $t \in [\tau_{i-1}, \tau_i]$ from the initial condition $\mathbf{x}_{i-1}$ is represented as the operator:

$$\phi(\mathbf{x}_{i-1}, \mathbf{u}_{i-1}) = \mathbf{x}_{i-1} + \int_{t_{i-1}}^{t_i} \boldsymbol{f}(\mathbf{x}(\tau), \mathbf{u}(\tau))d\tau. \tag{19}$$

This integral operator can be iterated for all specific forces and angular rates in $\mathbf{U}_k$ to propagate the state from t_{k-1} to t_k. The iterated integral operation is denoted as

$$\mathbf{x}_k = \boldsymbol{\Phi}(\mathbf{x}_{k-1}, \mathbf{U}_k). \tag{20}$$

Through mission scripting, multiple trajectory segments can be tied together to create a single complex 3D trajectory. Mission segments include: straight, accelerate, decelerate, climb, descent, turn, and several common aircraft aerobatic maneuvers. Each segment must specify segment duration, sample rate, velocity, altitude, heading, vertical rate (e.g. climb rate), and rotational rate (e.g turn rate, or aerobatic maneuver rate). Alternatively, way-point navigation may be specified, with segment distances and way-point actions (e.g. orbit, fly-through, fly-around, etc.) such that rates and accelerations are derived prior to generating ground truth.

For a specified trajectory, the ground truth states of the navigating vehicle, noise corrupted IMU measurements of specific forces and angular rates, and noise corrupted GNSS pseudoranges, Doppler and carrier phase to all-in-view satellites are each generated and saved to a file for later analysis.

Sensor errors and characteristics (e.g. data-rate) are either user specified, using data from a manufacturer datasheet, or pre-defined and selectable.

Each pre-defined sensor model was validated against commercial-off-the-shelf (COTS) signal generators, as well as real sensor data under controlled motion, e.g. linear rail, rate table, and stationary. Thus for any desired 3D trajectory, a complete set of realistic synthetic measurements is available for evaluation.

A. Signal Generation of a Turn Segment

To generate a turn segment, the initial position, velocity and attitude rotation matrix must be provided, as well as the total turn angle and the time increment. The input, initial calculations, and output are summarized in Table III-A

TABLE III

Input	
p_0	Initial position $(m) \in \mathbb{R}^3$
v_0	Initial velocity $(m/s) \in \mathbb{R}^3$
$R_n^b(0)$	Initial angle rotation matrix $(rad) \in \mathbb{R}^{3\times3}$
Ω	Total turn angle $(rad) \in \mathbb{R}^1$
dt	Time increment $(s) \in \mathbb{R}^1$
Initial Calculations	
$[\phi, \theta, \psi]^\intercal = R2euler(R_n^b(0))$	Convert rotation matrix to Euler angles
$a_\omega = \lvert 9.81 \tan\phi \rvert$	Centripetal acceleration
$r = \frac{\lVert v_0 \rVert_2^2}{a_\omega}$	Turn radius
$\omega = \frac{\lVert v_0 \rVert}{r}$	Turn rate
$n = \frac{\lVert \Omega \rVert}{\omega \cdot dt}$	Number of points to generate
$\lambda = -\text{sign } \psi \cdot \Omega \cdot \frac{1}{n}$	Angle increment
$v_\omega = \text{atan2}(v_0(2), v_0(1))$	Velocity angle
$\beta = v_\omega - \frac{\pi}{2} \cdot \text{sign } \phi$	(const.)
$\alpha(1) = p_0 + r \cdot \cos\beta$	(const.)
$\alpha(2) = p_0 + r \cdot \sin\beta$	(const.)
Output	
p	Trajectory position $(m) \in \mathbb{R}^{n\times3}$
v	Trajectory velocity $(m/s) \in \mathbb{R}^{n\times3}$
a	Trajectory acceleration $(m/s^2) \in \mathbb{R}^{n\times3}$
R_n^b	Trajectory rotation matrix $(rad) \in \mathbb{R}^{n\times9}$

The trajectory is integrated by Algorithm 1

Algorithm 1 Trajectory Integration for Turn Segment

$\Lambda = 0$;
for $i = 1 : n$ **do**
  Update cumulative angle:
  $\Lambda = \Lambda + \lambda$;
  Update position:
  $p_{i+1}(1) = \alpha(1) + r \cdot \cos(\beta - \pi + \Lambda_{i+1})$;
  $p_{i+1}(2) = \alpha(2) + r \cdot \sin(\beta - \pi + \Lambda_{i+1})$;
  $p_{i+1}(3) = p_i(3)$;
  Update velocity:
  $v_{i+1} = v_i \cdot R_n^{b\intercal}$;
  Update acceleration:
  $a_{i+1}(1) = a_\omega \cdot \frac{\alpha(1) - p_{i+1}(1)}{\lVert \alpha(1) - p_{i+1}(1) \rVert}$;
  $a_{i+1}(2) = a_\omega \cdot \frac{\alpha(2) - p_{i+1}(2)}{\lVert \alpha(2) - p_{i+1}(2) \rVert}$;
  $a_{i+1}(3) = 0$;
  Update rotation matrix:
  $\psi = \psi + \lambda$;
  $R_n^b(i+1) = euler2R([\phi, \theta, \psi]^\intercal)$;
end for

REFERENCES

[1] Seiko-Epson, "M-G320PDxx Inertial Measurement Unit (IMU) Data Sheet", M-G320PDxx datasheet, 2014 [Revised Oct. 31, 2014]. 1

[2] Gelb, A., *Applied Optimal Estimation*, The MIT Press, 2001.

[3] Farrell, J. A., *Aided Navigation: GPS with High Rate Sensors*, McGraw Hill, 2008. 3

[4] IEEE Std. 1293, *IEEE Standard Specification Format Guide and Test Procedure for Linear, Single-Axis, Non-gyroscopic Accelerometers*, 1998. 1

[5] Allan, D. W., *Statistics of atomic frequency standards*, Proceedings of the IEEE, 54(2), pp. 221230, 1966.

[6] Van Dierendonck, A.J, McGraw,J.B., *Relationship Between Allan Variance and Kalman Filter Parameters*, Proceedings of the Sixteenth Annual Precise Time and Time Interval (PTTI) Applications and Planning Meeting, Greenbelt, MD, 27-29 Nov 1984.

[7] Brown, R.G., *Kalman Filter Modeling*, Proceedings of the Sixteenth Annual Precise Time and Time Interval (PTTI) Applications and Planning Meeting, Greenbelt, MD, 27-29 Nov 1984.

[8] Carpenter, R., Lee, T., *A Stable Clock Error Model using Coupled First and Second-Order Gauss-Markov Processes*, NASA Technical Reports, AAS 08-109.

[9] Rogers, R. M., *Applied Mathematics in Integrated Navigation Systems*, AIAA Education Series, 2nd Ed., Reston, VA, 2003.

[10] R. A. Snay and M. Tomas Soler, *Continuously operating reference station (CORS): History, applications, and future enhancements,* Journal of Surveying Engineering, vol. 134, no. 4, 2008. 2

[11] Gurtner, W. *RINEX: The Receiver Independent Exchange Format Version 2.10,* Astronomical Institute, University of Berne, 10 December 2007 2